VOL. 19, NO. 20, OCTOBER 2024 ISSN 1819-6608
ARPN Journal of Engineering and Applied Sciences

www.arpnjournals.com

OPTIMIZED ACOUSTIC SIGNAL DENOISING USING MODIFIED THRESHOLD SHRINKAGE FUNCTIONS

Ausama Khalid and Yasin Al-Aboosi
Department of Electrical Engineering, Faculty of Engineering, Mustansiriyah University, Baghdad, Iraq
E-Mail: asamaw.khalid@uomustansiriyah.edu.iq

ABSTRACT

Underwater noise is a significant issue that affects various underwater activities such as ocean exploration, submarine communication, SONAR detection, etc. De-noising stages are traditionally embedded in underwater activities; therefore, developing de-noising algorithms is a highly demanded field of study. In this paper, a suggested modification is applied to some well-known threshold functions that will be used in conjunction with complex wavelet transform (CWT). The modification is applied to the Garrote threshold function and two semi-soft threshold functions. CWT is used to decompose the signals, that are corrupted by measured underwater noise, then a modified wavelet shrinkage is applied to remove the noise and recover the original signal. The performance of the modified functions is compared with the original functions and the soft threshold function. The results demonstrate that the functions after the modification have better performance than the soft function and the original functions. The Garrote function has about 2.5 dB signal-to-noise ratio improvement and the semi-soft functions also have about 2 dB and 0.5 dB improvement respectively.

Keywords: acoustic signal, complex wavelet, modified threshold functions, signals de-noising, threshold function, underwater noise.

Manuscript Received 31 August 2024; Revised 6 November 2024; Published 22 December 2024

INTRODUCTION

An underwater communication channel (UWC) is a challenging environment for the researcher, due to its time-varying characteristics, high attenuation, and high Doppler effect, which all generate a cumulative effect on such a channel that causes the UWC to be limited in bandwidth and transmission distance [1]. Due to high attenuation, the preferred type of signal in UWC is the acoustic signal [2]. However, UWC is also severely affected by a noise containing high non-Gaussian components due to the impulsive behavior of the noise especially in shallow water channels [3]. Underwater acoustic noise (UWAN) is one of the challenging types of noise that causes performance degradation in UWC systems [4], [5]. Thus there is an urgent need to improve the UWC systems.

Signal de-noising is an essential step in various signal processing applications, including image processing, speech recognition, signal detection, and communication systems. The main objective of signal de-noising is removing the unwanted noise without affecting the underlying information [6]. The majority of communication systems and signal processing systems assume the noise as additive white Gaussian noise (AWGN), which is valid in most cases [7]. However, in some communication channels, the assumption of AWGN is not accurate to describe the noise in some channels such as underwater channels [8]. The power of colored noise will be distributed over the frequency spectrum unequally; therefore the noise power will be higher at certain frequencies and lower at other frequencies [9]. To remove a colored noise, such as UWAN, it was suggested to use a pre-whitening step to convert the noise into white noise by using a linear prediction filter [4]. Or, by applying multi-level de-noising algorithms as suggested by Y. Al-Aboosi & A. Sha'ameri [9], and Aggrawal & Singh *et al*. [10].

One of the widely used yet efficient methods in the de-noising process is wavelet shrinkage, it has been extensively used as a de-noising method for images and audio signals [11], [12]. Some researchers proposed a wavelet de-noising method that required prior knowledge about the noise that the system is utilized to remove [13]. Others adopted methods that required no prior knowledge about the noise by utilizing a method to calculate the threshold without knowing the noise characteristics such as [15], [10]. Two parts are needed to properly apply the wavelet shrinkage, threshold estimation method, and thresholding functions. Many threshold functions are used to eliminate, with the help of a computed threshold, unwanted noise without affecting the desired information such as soft and hard thresholds [14], semi-soft functions [15], and the Garrote function [16]. The wavelet normally has some limitations such as shift sensitivity and poor directionality [17], thus the researchers solved these limitations by replacing the normal wavelet with a complex wavelet [18], [19]. The complex wavelet is increasingly used in image and signal denoising for its desired properties [20], [21]. The previous studies either modified the threshold estimation method [10] or introduced a new threshold function [22].

This paper proposes a modification to three threshold functions and studies the effect of this modification on its performance. Complex wavelet transform is utilized in this study. The threshold functions will be tested in removing a colored non-gaussian UWAN noise. The performance was evaluated using two criteria: root mean squared error (RMSE) and signal-to-noise ratio (SNR). The effectiveness of the modified threshold

functions is compared with the widely used soft threshold function. The obtained results demonstrate that, when applied in the de-noising process, the suggested approach achieved better enhancement when compared with the original form of the Garrote function, and Semi-soft functions in addition to the soft threshold function.

The rest of this paper is organized as; section 2 describes complex wavelet transform and UWAN noise model. Section 3 presents the utilized threshold functions. Section 4 introduces the modified threshold functions. Section 5 describes the performance evaluation, results, and discussion. Section 6 briefly concludes the conducted study.

SIGNAL TRANSFORM AND NOISE MODEL

Complex Wavelet Transform

Normal discrete wavelet transform (DWT) uses a small locally oscillating signal called a wavelet, using that small signal gives the ability to extract frequency information from the signal of interest. Wavelet signal has two key parameters: dilation or time shift to extract information for any given time from the signal of interest and scale which is a frequency-dependent parameter. For a high frequency, the wavelet signal narrows giving a low-frequency resolution and for a low frequency, the wavelet signal widens giving a high-frequency resolution [17]. But DWT has some major drawbacks such as poor directionality and shift variant sensitivity [18], [17]. To solve these disadvantages, researchers are increasingly using a Complex Wavelet transform (CWT) alternative to DWT. CWT is implemented using two parallel filter banks. The filters in this structure are built in such a manner that the subbands of the top tree are understood as the real part of the CWT and the bottom tree as the imaginary part [23]. The two filters form a Hilbert transform pair, as shown in (1):

$$\eta_{im} = H\{\eta_{re}\} = -j * sgn(\omega) * \eta_{re} \quad (1)$$

Where η_{re} and η_{im} are the Fourier transform of the response of real and imaginary filters respectively. The filter bank structure of CWT for three levels is shown in Figure-1. Although CWT introduces a redundancy by a factor of 2 in one dimension and needs more memory, it overcomes the problem of shift sensitivity. It can properly decompose complex signals [11].

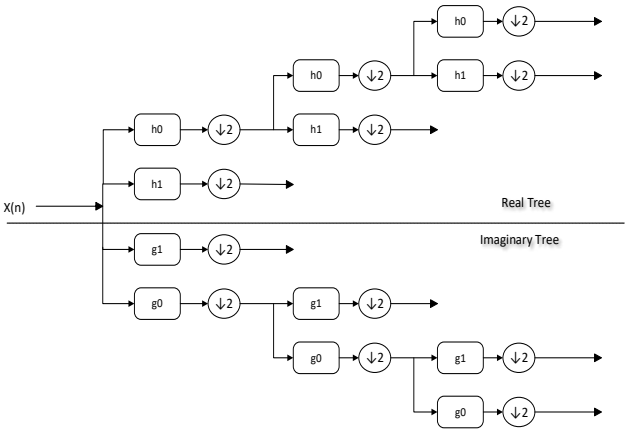

Figure-1. CWT Filter bank implementation [11].

To satisfy (1) the filters are supposed to meet some properties such as the approximate half-sample property as shown in (2), the perfect reconstruction (orthogonal or biorthogonal), the finite support (FIR filters), the good stop band, and the linear phase [18], [19]. If h0, and g0 are the responses of the lowpass filters in real and imaginary trees then:

$$g0 = h0\left(n - \frac{1}{2}\right) \quad (2)$$

UWAN Noise

The UWAN is a noise that depends on the frequency and its power decreases with frequency increase [4], [23], and [25]. Figure-2 demonstrates the power spectral of a measured noise for various depths. The previous studies proved that UWAN is a non-gaussian noise; it rather follows a statistical distribution known as student t-distribution [24], [26], and [27].

The autocorrelation of Gaussian noise is a delta Dirac function indicating i.i.d distribution [7]. However, after analyzing the noise samples, the autocorrelation also indicates that the noise has side lobes which is a property of colored noise. Figure-3, below gives the noise samples and their autocorrelations.

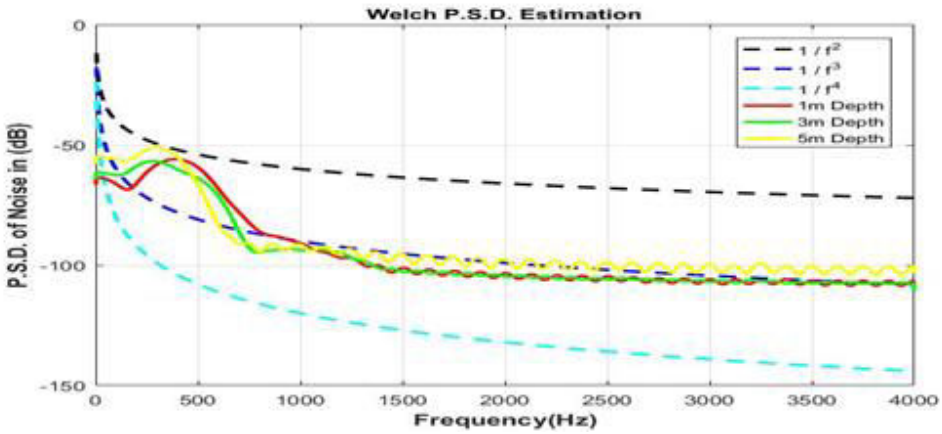

Figure-2. The power spectral density of UWAN [11].

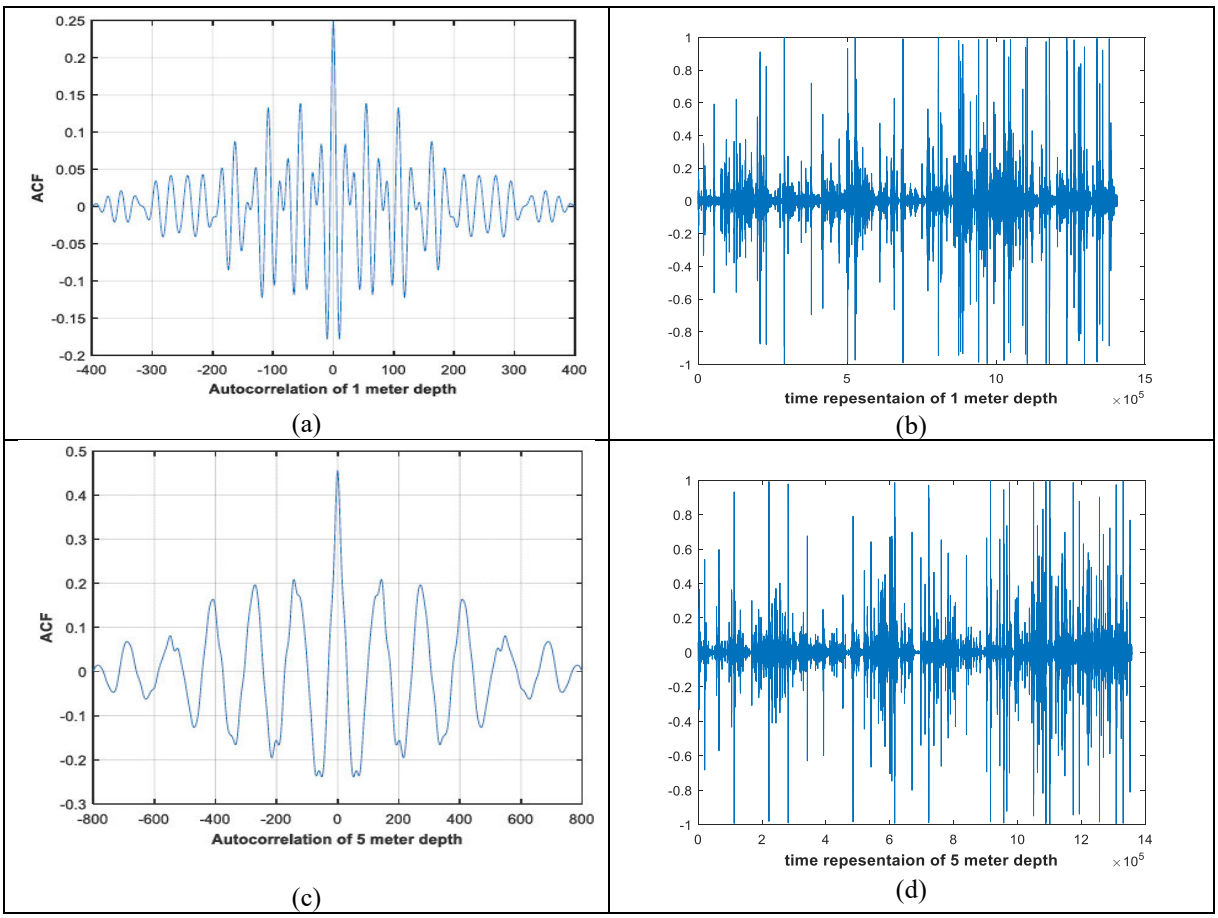

Figure-3. The noise samples and the autocorrelation function for (a) 1m, and (b) 5m depths [27].

Threshold Functions

Wavelet shrinkage reduces noise by thresholding wavelet (details) coefficients according to a threshold function. To apply wavelet shrinkage, two important factors are required: threshold value and threshold function. The widely used threshold estimation presented by D. Donoho in [14]. Threshold estimation is given in (3):

$$Th = \sigma_k \sqrt{2Log(N)} \quad (3)$$

Equation (3) gives the threshold for the signal of length N. Where σ denotes the noise standard deviation for a specific level. Donoho suggested a robust method to calculate the standard deviation by using the median value of the details coefficients because the details coefficients are mostly noise. Despite, the fact that the details coefficients contain noise, some of the signal is presented

in the details. Therefore, σ is divided by factor 0.6745 making the function as given below [14]:

$$\sigma_k = \frac{median(|X_d(n,k)|)}{0.6745} \quad (4)$$

Where X_d is the detailed coefficients at a specific level. Since the DT-DWT is used as an alternative to DWT the produced details from both trees can be written as [18]:

$$X_d(n,k) = X_{d,re}(n,k) + jX_{d,im}(n,k) \quad (5)$$

Then the magnitude of (5) is taken and substituted in (4) to obtain the standard deviation.

After computing the proper threshold, the next step is to apply that threshold using a threshold function. The threshold will be applied separately for the real tree and the imaginary tree in our case for each level. The most common methods used in wavelet shrinkage are as follows:

- Soft threshold: in this method, every high-value coefficient will be attenuated by the threshold. The low-value coefficient will be set to zero. This method makes the output signal a lot smoother and reduces discontinuity in the thresholded coefficients [10], [15].

$$X_{d,Th} = \begin{cases} sgn(X_d)(|X_d| - Th) & X_d \geq Th \\ 0 & X_d < Th \end{cases} \quad (6)$$

- Garrote threshold: this method was first introduced as a de-noising method in [16], and used in speech enhancement [22]. It performs a hard threshold for signals with high values and softens the signals with low data values [16]. The garrote function is a compromise between hard and soft threshold functions. The garrote function is given below:

$$X_{d,Th} = \begin{cases} \left(|X_d| - \frac{Th^2}{|X_d|}\right) & X_d \geq Th \\ 0 & X_d < Th \end{cases} \quad (7)$$

- Semi-soft threshold: this method is a type of nonlinear threshold function. It was proposed to overcome some problems introduced in earlier-mentioned functions [22], [11]. In a soft threshold, there is a constant difference between the input and the output signal [16]. Garrote has a constant deviation in the output signal regarding the input signal [22]. Two thresholds are used in this function primary threshold (Upper) and secondary threshold (lower). The primary threshold is calculated using the universal threshold estimation mentioned earlier and the secondary threshold is derived from the primary [11]. This method sets small value samples to zero, shrinks moderate values by a specific nonlinear function, and retains large value samples. Two functions will be considered in this study, these functions are named after the corresponding authors to distinguish between the two functions.

a) Raj semi-soft function: The method introduced a secondary threshold that can be calculated from the main threshold as [11]:

$$Th1 = Th * m \quad (8)$$

Where m is a factor that takes a value from 1 to Inf. If (m = 1), this threshold method will perform a hard thresholding, if (m = ∞), this method will perform a soft thresholding [11]. The Raj semi-soft is expressed as:

$$X_{d,Th} = \begin{cases} X_d & |X_d| > Th1 \\ \frac{Th1(X_d - Th)}{Th1 - Th} & Th < |X_d| \leq Th1 \\ 0 & |X_d| \leq Th \end{cases} \quad (9)$$

b) Shau semi-soft function: In this method, the secondary threshold is calculated via initial silence regions [22]. Equation (8) will be considered as a replacement for the original method of calculating the secondary threshold. It resolves the discontinuity of the hard thresholding and the constant difference represented by soft thresholding. The Shau semi-soft function is written as:

$$X_{d,Th} = \begin{cases} X_d & |X_d| > Th1 \\ \frac{X_d^3}{Th1^2} & Th < |X_d| \leq Th1 \\ 0 & |X_d| \leq Th \end{cases} \quad (10)$$

The hard threshold method will not be considered in this study as its performance is less than any other mentioned method [10], [11], [22]. Figure-4 below shows a linear test of the threshold methods. Figure-4(a) illustrates the constant difference between input and output signals presented by soft thresholding. Figure-4(b) shows a Garrote threshold, where the difference between the input and the output signal is decreased [22]. Figure-4(c) shows a Raj semi-soft in which the high-value samples are retained and there is a smoother discontinuity at low-value samples [11]. Also, Figure-4(d) shows Shau semi-soft where the samples gradually approach zero at the threshold point given a much smoother discontinuity.

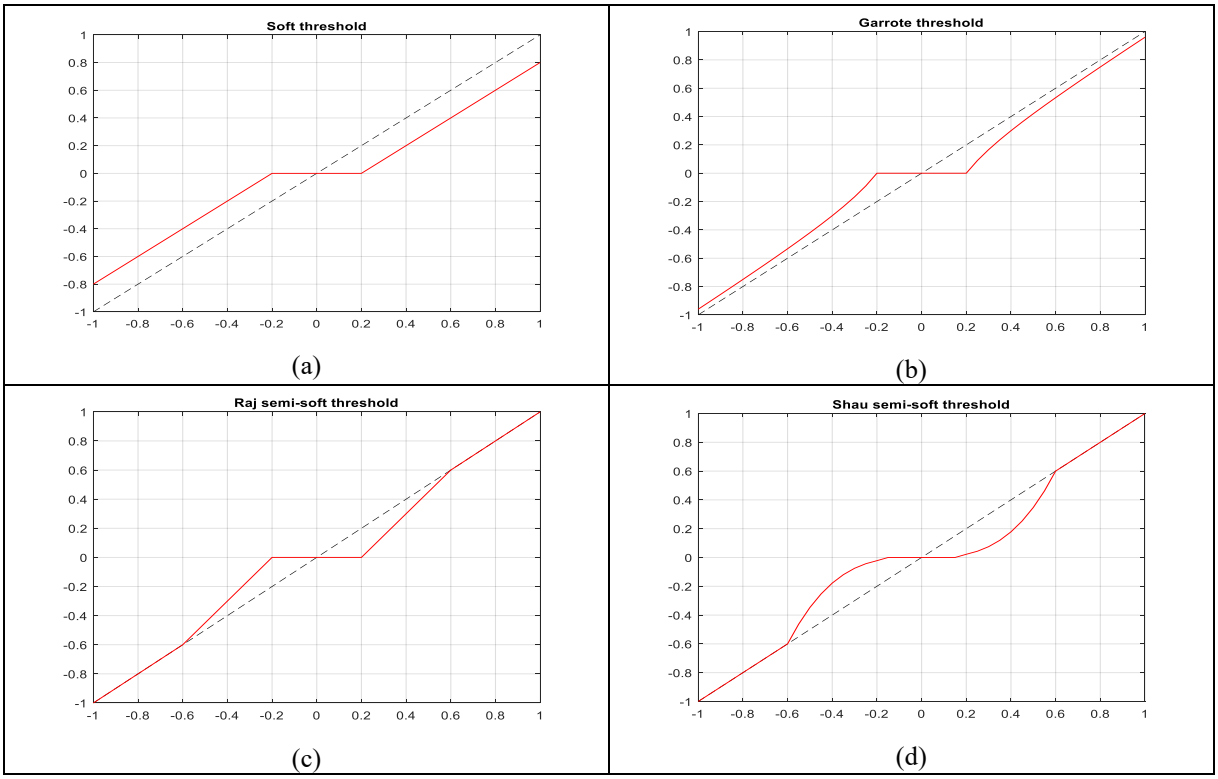

Figure-4. The output results of (a) soft, (b) Garrot, (c) Raj semi-soft, and (d) Shau semi-soft threshold functions, for linear input tests.

Modified Threshold Functions

The early studies proved that the details coefficient contains not only noise but some part of the important information also exists with that noise [15], [28]. Although wavelet shrinkage using various threshold functions has proved its ability to efficiently remove the noise from signals corrupted by noise, some of the noise will persist especially UWAN noise which has an impulsive behavior that makes it harder to be removed [24]. In this paper, a factor b will be added to the Garrote, Raj semi-soft, and Shau semi-soft threshold functions. This factor will help improve the performance by further removing the remaining noise. The value of this factor is ($0.1 \leqslant b \leqslant 1$) which controls how much of the thresholded samples are kept for the output signals. The effect of adding this factor was proved using MATLAB simulations, the obtained results are listed in section 6. The threshold function after adding the factor will be expressed as:

- Modified Garrote threshold function:

$$X_{d,Th} = \begin{cases} b * \left(|X_d| - \frac{Th^2}{|X_d|}\right) & X_d > Th \\ 0 & X_d \leq Th \end{cases} \quad (11)$$

- Modified Raj semi-soft threshold function:

$$X_{d,Th} = \begin{cases} X_d & |X_d| > Th1 \\ b * \frac{Th1(X_d - Th)}{Th1 - Th} & Th < |X_d| \leq Th1 \\ 0 & |X_d| \leq Th \end{cases} \quad (12)$$

- Modified Shau semi-soft threshold function:

$$X_{d,Th} = \begin{cases} X_d & |X_d| > Th1 \\ b * \frac{X_d^3}{Th1^2} & Th < |X_d| \leq Th1 \\ 0 & |X_d| \leq Th \end{cases} \quad (13)$$

The effect of the added factor in the case of garrote can increase the difference between input and output signals indicating the thresholding process of the higher value samples, that contain information and noise, removes more noise from it. In the case of the Raj and Shau semi-soft functions the effect of b factor when decreasing the value of b becomes approximately similar in both functions. Shau and Raj's semi-soft functions have an increasing difference between input and output signals in a moderate values range when decreasing b. Figure-5 shows the effect of adding the b factor on the results of the linear test of the threshold functions when b=0.6. In Figure-5(b, c) a discontinuity becomes noticeable near the secondary threshold for the Shau and Raj semi-soft threshold.

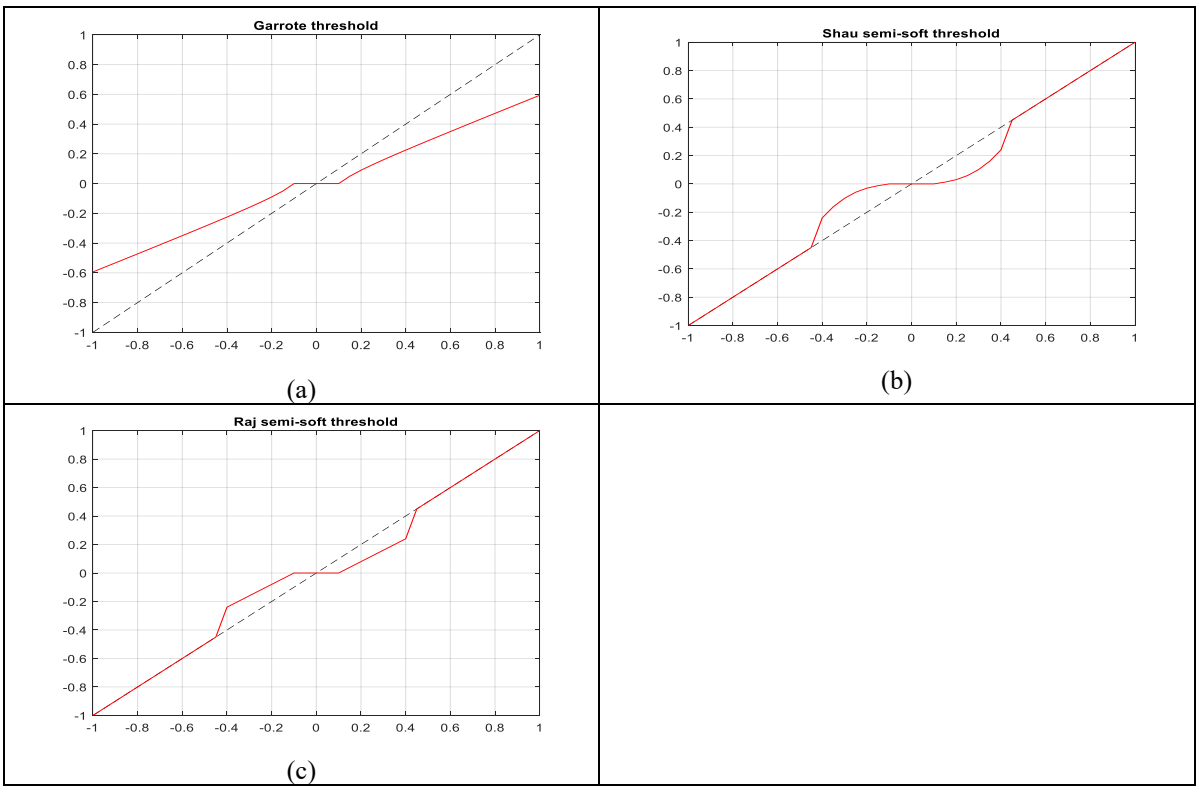

Figure-5. The obtained results of the modified (a) Garrot, (b) Shau semi-soft, and (c) Raj semi-soft threshold functions, for linear input test with b = 0.6.

Simulation Results

Try The earlier mentioned samples of real collected data of UWAN were used to validate each of the thresholding methods. The data were collected from the Tigris River for three levels 1 meter, and 5 meter [25], [27]. The sampling frequency was 8000 Hz. The input SNRs are 4.05 dB, 3.25 dB, and 3.29 dB for 1m, 3m, and 5m depths respectively. Two performance measurements are used to assess the improvement in the threshold functions performance with the added factor SNR and RMSE.

The simulation is done using two types of signals, and each of those signals will be corrupted with the non-Gaussian UWAN noise. These signals include a single-frequency signal and a variable-frequency Chirp signal. The chosen level of decomposition for CWT is 4 levels. CWT filter functions can be found in [17] and [18]. The simulation can be summarized as:

- Passing each corrupted speech signal to CWT transform to obtain the details and the approximation coefficients.
- By applying (3) to the obtained details coefficients to find the threshold at every level of decomposition. The obtained threshold is then used with each threshold function to remove the noise from the details coefficients.
- By using the thresholded details and the original approximation, reconstruct the de-noised signal.
- During the threshold process the value of b is changed gradually to highlight the effect of that factor on each threshold function.

Performance Evaluation

The performance is evaluated using some indices to demonstrate the effectiveness of the algorithms. Two widely utilized methods are used for testing the quality of the signals: RMSE and SNR [9].

- The root mean squared error (RMSE) is a method that measures the similarity between the clean and the de-noised signal. If RMSE is lower after the de-noising process the signal has been improved. It is calculated using:

$$RMSE = \sqrt{\frac{1}{N}\sum\left(s(n) - \tilde{s}(n)\right)^2} \quad (14)$$

Where s(n) represents the clean signal and $\tilde{s}(n)$ is the signal after removing the noise.

- The SNR is the ratio between the signal power and the noise power. SNR is expressed in dB. The higher SNR means the signal is more than the noise. SNR is given as:

$$SNR = 10\log\left(\frac{\sum s(n)^2}{\sum\left(s(n)-\tilde{s}(n)\right)^2}\right) \quad (15)$$

RESULTS AND DISCUSSIONS

By setting the threshold level and threshold function, the number of decomposition levels in the wavelet threshold denoising method also affects the quality of the reconstructed signal. To improve denoising, more decomposition levels are needed, which will increase processing and calculation times. Thresholding is used to quantify the detail coefficients at each level of decomposition. This might result in an excessively high reconstruction error and worse signal quality. The simulation is conducted on two signals with noise at three depths. The resulting SNR and RMSE values are presented in the tables below for each signal. The input and the output SNR and RMSE, in dB, are shown in every case using the modified threshold functions and the soft threshold function. The soft threshold SNR and RMSE values remain constant, due to no modification is applied to the soft threshold function. The value of b is changed to observe its effect on the modified threshold functions. It is noted that there is a major improvement when the value of b approaches 0.1.

a) Chirp signal

The first simulation is done using a linear frequency Chirp signal which was corrupted by UWAN noise for three depths. Table-1 gives the SNR results of de-noising of 1m depth UWAN noise. Garrote threshold has the poorest performance when the effect of b is removed; in contrast, Garrote has the best performance when decreasing the value of b. The Shau threshold function has a stable performance compared to the other functions with a minimum increase in SNR. The Raj Threshold function, on the other hand, shows improved performance. Table-2 also shows the results of RMSE for 1m noise. The best performance is in the Garrote threshold and the stable performance is the Shau threshold.

Table-1. SNR results for 1m depth UWAN in db.

SNR input	Soft	b	Garrote	Raj_Semi_soft	Shau_Semi_soft
4.05	7.01	0.1	8.23	7.44	7.48
4.0.5	7.01	0.2	8.16	7.38	7.47
4.05	7.01	0.3	8.06	7.3	7.45
4.05	7.01	0.4	7.92	7.23	7.43
4.05	7.01	0.5	7.74	7.14	7.4
4.05	7.01	0.6	7.53	7.05	7.38
4.05	7.01	0.7	7.3	6.96	7.36
4.05	7.01	0.8	7.05	6.86	7.33
4.05	7.01	0.9	6.78	6.76	7.3
4.05	7.01	1	6.5	6.65	7.28

Table-2. RMSE results for 1m depth UWAN.

RMSE Input	Soft	b	Garrote	Raj_Semi_soft	Shau_Semi_soft
0.0266	0.0189	0.1	0.0165	0.018	0.0179
0.0266	0.0189	0.2	0.0166	0.0181	0.018
0.0266	0.0189	0.3	0.0168	0.0183	0.018
0.0266	0.0189	0.4	0.0171	0.0185	0.018
0.0266	0.0189	0.5	0.0174	0.0186	0.0181
0.0266	0.0189	0.6	0.0178	0.0188	0.0181
0.0266	0.0189	0.7	0.0183	0.019	0.0182
0.0266	0.0189	0.8	0.0188	0.0193	0.0182
0.0266	0.0189	0.9	0.0194	0.0195	0.0183
0.0266	0.0189	1	0.0194	0.0197	0.0184

Figure-6 demonstrates the results of a comparison between the soft threshold and each of the threshold functions with and without the modification, setting b=0.1, in terms of output SNR for the process of de-noising a 5m depth noise vs input SNR, in dB. Figure-7 also shows the result of the same comparison in terms of RMSE vs input SNR in dB, the results of RMSE are inverted for clear results. All the threshold methods show an improved performance by utilizing the b factor. It is noted that the Shau semi-soft gave a stable and improved performance, the Raj semi-soft showed improved performance, and the Garrote also showed improved performance. The RMSE results indicate that the performance of the three threshold methods is approximately similar. Removing the effect b by setting it to 1, the Garrote gives the poorest performance.

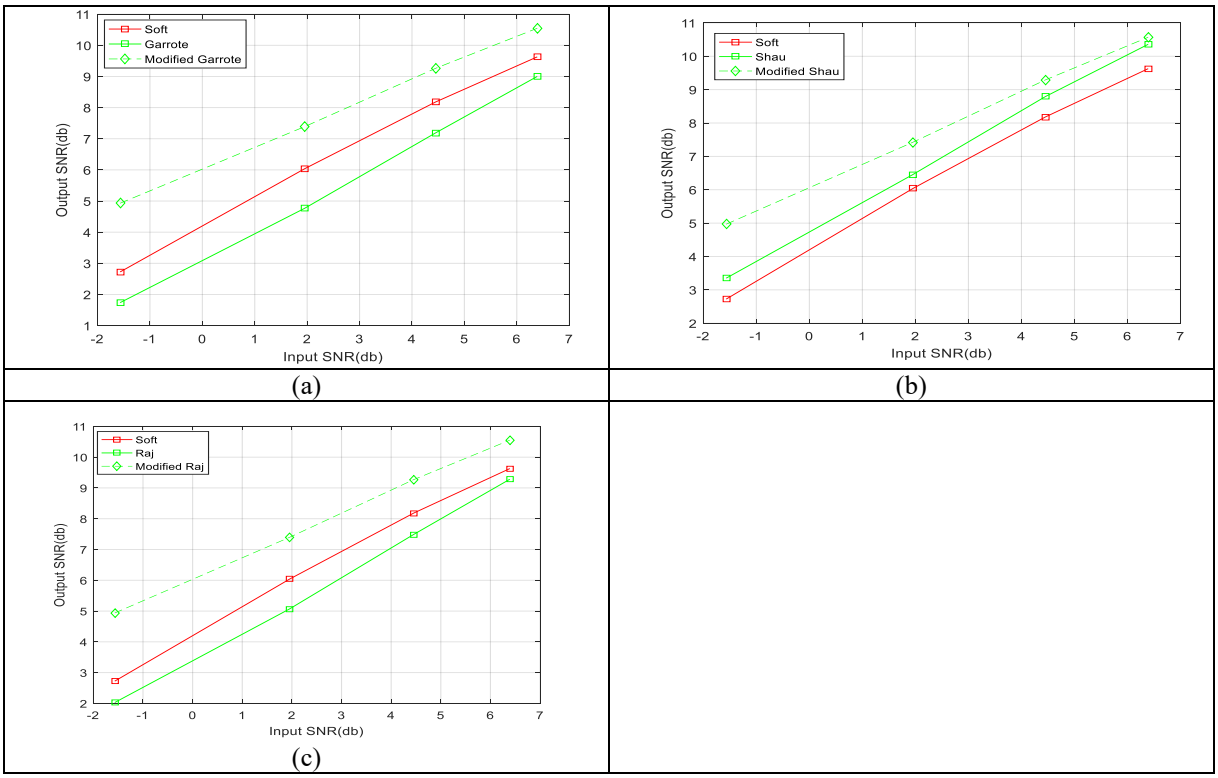

Figure-6. Results of SNR comparison between soft (solid red), modified function (dashed green), and original function (solid green) using (a)Garrote, (b)Shau semi-soft, and (c)Raj semi-soft functions with 5m depth noise and $b = 0.1$ (chirp signal).

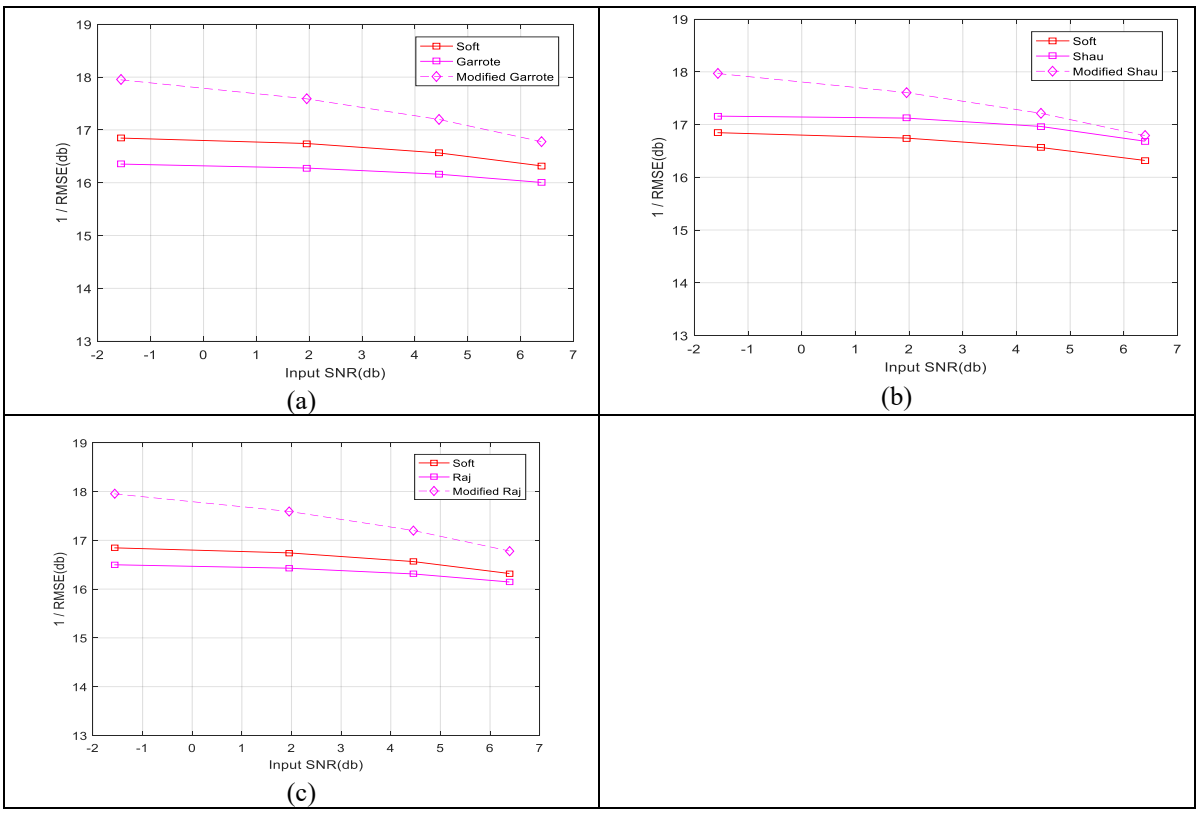

Figure-7. Results of RMSE comparison between soft (solid red), modified function (dashed purple), and original function (solid purple) using (a)Garrote, (b)Shau semi-soft, and (c)Raj semi-soft functions with 5m depth noise and $b = 0.1$ (chirp signal).

b) Single tone

The second simulation is done using a single-frequency signal that was also corrupted by the same UWAN noise. Tables-3, Table-4 shows the result of SNR and RMSE of the de-nosing process for 1m depth. It is observed that there is a small improvement in the Shau threshold function. The Garrote output SNR and RMSE are improved, as well as in the case of the Raj threshold function, there is an improvement. Although the Garrote threshold showed the poorest performance without the modification, the Garrote threshold gives the highest performance with the added modification.

Table-3. SNR results from 1m depth UWAN in db.

SNR input	Soft	b	Garrote	Raj_Semi_soft	Shau_Semi_soft
4.06	7.33	0.1	8.57	7.73	7.77
4.06	7.33	0.2	8.5	7.67	7.75
4.06	7.33	0.3	8.4	7.6	7.73
4.06	7.33	0.4	8.26	7.53	7.71
4.06	7.33	0.5	8.08	7.45	7.69
4.06	7.33	0.6	7.87	7.36	7.67
4.06	7.33	0.7	7.64	7.27	7.64
4.06	7.33	0.8	7.39	7.18	7.62
4.06	7.33	0.9	7.11	7.08	7.59
4.06	7.33	1	6.83	6.97	7.56

Table-4. RMSE results from 1m depth UWAN.

RMSE Input	Soft	b	Garrote	Raj_Semi_soft	Shau_Semi_soft
0.0266	0.0182	0.1	0.0158	0.0174	0.0173
0.0266	0.0182	0.2	0.0159	0.0175	0.0174
0.0266	0.0182	0.3	0.0161	0.0177	0.0174
0.0266	0.0182	0.4	0.0164	0.0178	0.0175
0.0266	0.0182	0.5	0.0167	0.018	0.0175
0.0266	0.0182	0.6	0.0171	0.0182	0.0175
0.0266	0.0182	0.7	0.0176	0.0184	0.0176
0.0266	0.0182	0.8	0.0181	0.0186	0.0177
0.0266	0.0182	0.9	0.0187	0.0188	0.0177
0.0266	0.0182	1	0.0193	0.019	0.0178

The presented results in Figure-8, and Figure-9, demonstrate an output SNR and RMSE, in dB, comparison results of the soft threshold function and the modified threshold functions with and without the modification using 5m depth noise. The results of RMSE are inverted in Figure-9, to remove the sign. There is an enhancement in the performance for all threshold functions. It is observed that the Shau semi-soft function has a minimum improvement while The Garrote and Raj semi-soft functions have a significant improvement. As the value of b approaches 1, the performance of Garrote and Raj's semi-soft threshold is reduced and becomes less than the soft threshold. The unmodified Garrote shows the poorest performance while the unmodified Shau semi-soft shows a high performance.

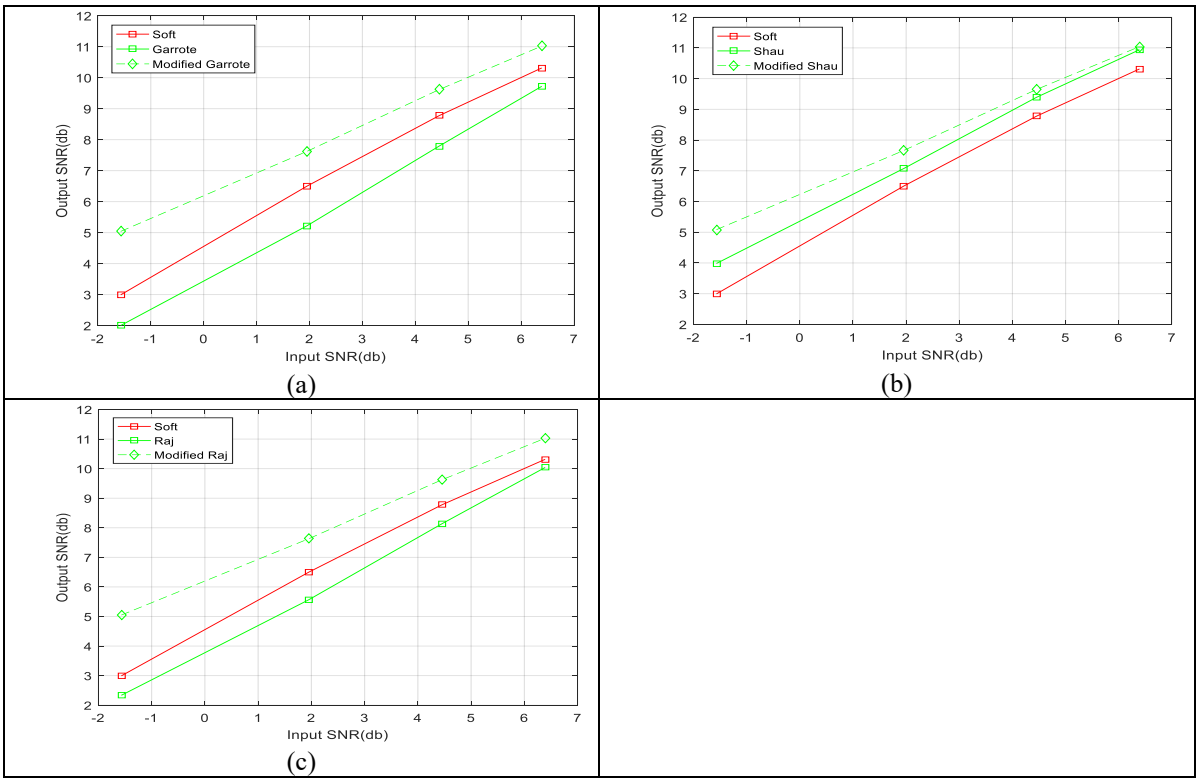

Figure-8. Results of SNR comparison between soft (solid red), modified function (dashed green), and original function (solid green) using (a)Garrote, (b)Shau semi-soft, and (c)Raj semi-soft functions with 5m depth noise and $b = 0.1$ (single frequency).

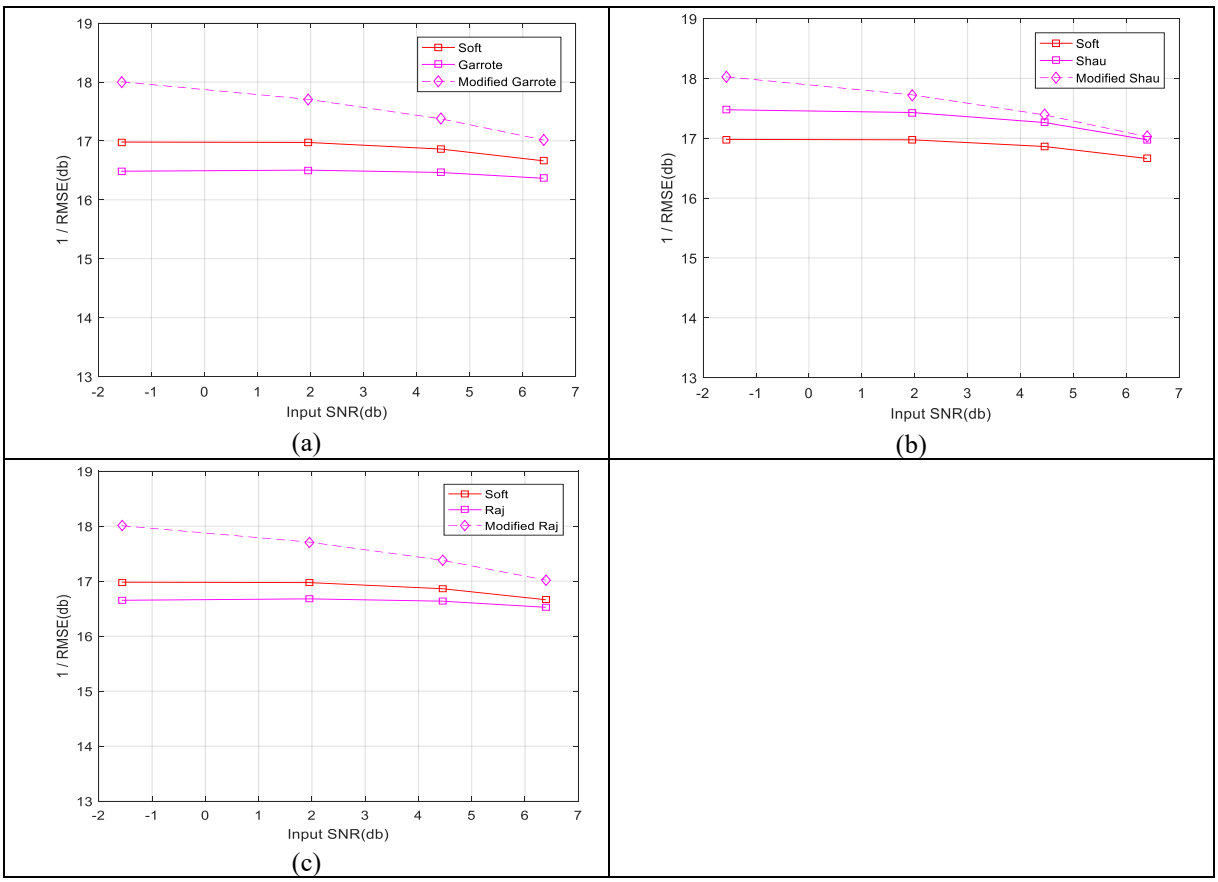

Figure-9. Results of RMSE comparison between soft (solid red), modified function (dashed purple), and original function (solid purple) using (a)Garrote, (b)Shau semi-soft, and (c)Raj semi-soft functions with 5m depth noise and $b = 0.1$ (single frequency).

CONCLUSIONS

In this paper, a proposed modification to three thresholding functions, Garrote, and two different semi-soft functions is studied and a comparison is made between the modified functions performance and soft thresholding. The performance was analyzed using signal-to-noise ratio (SNR) and root mean squared error (RMSE). The de-noising was applied to two types of speech signals: single frequency and chirp signals corrupted by real collected underwater acoustic noise. Although the original Garrote has a lower performance compared to the soft threshold and other functions, its performance after the added modification demonstrates a superior performance than the other functions. The semi-soft threshold function presented by Shau produces a better performance than the soft function, however, the modified Garrote exceeds the Shau function's performance in terms of SNR and RMSE. The Garrote output SNR increased by approximately 2.5 dB. The semi-soft functions also show an improved performance compared to its original formulas. The semi-soft function presented by Raj shows increasing in SNR by around 2 dB and the Shau function has SNR improvement by around 0.5 dB. Likewise, the RMSE was reduced in all threshold functions. The lowest RMSE was observed with the use of the Garrote in most of the cases. All the modified threshold functions give a better performance than soft threshold functions for reduced values of the added factor.

Conflict of Interest

The authors declare that there are no conflicts of interest regarding the publication of this manuscript.

REFERENCES

[1] P. C. Etter. 2012. Advanced applications for underwater acoustic modelling. Advances in Acoustics and Vibration, 2012: 1-28, doi:10.1155/2012/214839.

[2] Burrowes G. & Khan J. Y. 2011. Short-range underwater acoustic communication networks. In InTech eBooks, doi: 10.5772/24098.

[3] A. Z. Sha'ameri, Y. Y. Al-Aboosi, and N. H. H. Khamis. 2014. Underwater acoustic noise characteristics of shallow water in tropical seas. Proc. Of the International Conference on Computer &

Communication Engineering 2014 (ICCCE 2014), doi:10.1109/iccce.2014.34

[4] S. Basagni, M. Conti, S. Giordano and I. Stojmenovic. 2013. Advances in Underwater Acoustic Networking. In Mobile ad hoc networking: Cutting Edge Directions. John Wiley & Sons, doi:10.1002/9781118511305.ch23.

[5] R. P. Hodges. 2011. Underwater acoustics: Analysis, Design, and Performance of Sonar. John Wiley & Sons.

[6] H. Hassanpour, A. Zehtabian, and S. J. Sadati. 2012. Time-domain signal enhancement based on an optimized singular vector denoising algorithm. Digital Signal Processing, 22(5): 786-794, doi:10.1016/j.dsp.2012.03.009.

[7] A. V. Oppenheim and G. C. Verghese, Signals, systems, and inference: Class Notes for 6.011, Introduction to Communication, Control, and Signal Processing. 2010.

[8] J. Panaro, F. Lopes, L. Barreira and F. Souza. 2012. Underwater acoustic noise model for shallow water communications. Anais De XXX Simpósio Brasileiro De Telecomunicações, doi:10.14209/sbrt.2012.85.

[9] Y. Y. Al-Aboosi and A. Z. Sha'ameri. 2017. Improved signal de-noising in underwater acoustic noise using S-transform: A performance evaluation and comparison with the wavelet transform. Journal of Ocean Engineering and Science, 2(3): 172-185, doi:10.1016/j.joes.2017.08.003.

[10] R. Aggarwal, J. K. Singh, V. K. Gupta, S. Rathore, M. Tiwari and A. Khare. 2011. Noise Reduction of Speech Signal using Wavelet Transform with Modified Universal Threshold. International Journal of Computer Applications, 20(5): 14-19, doi: 10.5120/2431-3269.

[11] V. N. P. Raj and T. Venkateswarlu. 2012. Denoising of medical images using dual-tree complex Wavelet Transform. Procedia Technology, 4: 238-244, doi:10.1016/j.protcy.2012.05.036.

[12] Y. Xu, J. B. Weaver, D. M. Healy, and J. Lu. 1994. Wavelet transform domain filters: a spatially selective noise filtration technique. IEEE Transactions on Image Processing, 3(6): 747-758, doi:10.1109/83.336245.

[13] M. Saeedzarandi, H. Nezamabadi-Pour and A. Jamalizadeh. 2019. Dual-Tree Complex WaVeLet coefficient magnitude modeling using scale mixtures of Rayleigh distribution for image denoising. Circuits Systems and Signal Processing, 39(6): 2968-2993, doi: 10.1007/s00034-019-01291-y.

[14] D. L. Donoho. 1995. De-noising by soft-thresholding. 1995. IEEE Transactions on Information Theory, 41(3): 613-627, doi:10.1109/18.382009.

[15] D. L. Donoho and I. M. Johnstone. 1994. Ideal spatial adaptation by wavelet shrinkage. Biometrika, 81(3): 425-455, doi:10.1093/biomet/81.3.425.

[16] H.-Y. Gao. 1998. Wavelet shrinkage denoising using the non-negative garrotte. Journal of Computational and Graphical Statistics, 7(4): 469-488, doi:10.1080/10618600.1998.10474789.

[17] Shukla P. 2003. Complex wavelet transforms and their applications. Ph.D. dissertation, Strathclyde Univ., Scotland, United Kingdom.

[18] W. Selesnick, R. G. Baraniuk and N. C. Kingsbury. 2005. The dual-tree complex wavelet transform. IEEE Signal Processing Magazine, 22(6): 123-151, doi:10.1109/msp.2005.1550194

[19] W. Selesnick. 2001. Hilbert transforms pairs of wavelet bases. IEEE Signal Processing Letters, 8(6): 170-173, doi:10.1109/97.923042.

[20] U. Bal. 2012. Dual tree complex wavelet transform based denoising of optical microscopy images," Biomedical Optics Express, 3(12): 3231, doi:10.1364/boe.3.003231.

[21] D. Bhonsle and S. Dewangan. 2012. Comparative Study of Dual-Tree Complex Wavelet Transform and Double Density Complex Wavelet Transform for Image Denoising Using Wavelet-Domain. Journal of Scientific and Research Publications, [Online]. Available: http://www.ijsrp.org/research_paper_jul2012/ijsrp-july-2012-56.pdf

[22] S. Sahu and N. Rayavarapu. 2023. Compressive speech enhancement using semi-soft thresholding and improved threshold estimation. International Journal of Power Electronics and Drive Systems/International Journal of Electrical and Computer Engineering, 13(3): 2788, doi:10.11591/ijece.v13i3.pp2788-2800.

[23] N. Kingsbury. 2001. Complex wavelets for shift invariant analysis and filtering of signals. Applied and Computational Harmonic Analysis, 10(3): 234-253, doi:10.1006/acha.2000.0343.

[24] Y. Y. Al-Aboosi, H. A. Taha, and H. A. Abdualnabi. 2018. Locally Optimal Detection of Signals in Underwater Acoustic Noise with Student's t-distribution. IOP Conference Series Materials Science and Engineering, 433: 012086, doi:10.1088/1757-899x/433/1/012086.

[25] M. S. Mahmood and Y. Y. Al-Aboosi. 2023. Effects of Multipath Propagation Channel in Tigris River. Journal of Engineering and Sustainable Development, 27(2): 256-271, doi:10.31272/jeasd.27.2.9.

[26] T. E. Murad and Y. Al-Aboosi. 2023. BIT Error Performance Enhancement for Underwater Acoustic Noise Channel by using Channel Coding. Journal of Engineering and Sustainable Development, 27(5): 659-670, doi:10.31272/jeasd.27.5.8

[27] Mahmood S. M. 2021. Modeling and Performance Analysis of an Underwater Acoustic Communication Channel Using Ray Model. M.S. thesis, Dept. Electric Eng., Mustansiriyah Univ., Baghdad, Iraq.

[28] Z. Zhou et al. 203. Improvement of the signal-to-noise ratio of Lidar echo signal based on wavelet de-noising technique. Optics and Lasers in Engineering, 51(8): 961-966, doi:10.1016/j.optlaseng.2013.02.011.